fractal and fractional

MDPI

Article

A Low Power Analog Integrated Fractional Order Type-2 Fuzzy PID Controller

Vassilis Alimisis *, Nikolaos P. Eleftheriou *, Evangelos Georgakilas, Christos Dimas, Nikolaos Uzunoglu and Paul P. Sotiriadis

Deptartment of Electrical and Computer Engineering, National Technical University of Athens, 10682 Athens, Greece; el16047@mail.ntua.gr (E.G.); chdim@central.ntua.gr (C.D.); nuzu@mail.ntua.gr (N.U.); pps@mail.ntua.gr (P.P.S.)
* Correspondence: alimisisv@mail.ntua.gr (V.A.); el19432@mail.ntua.gr (N.P.E.)

Abstract: This paper introduces an analog integrated fractional order type-2 fuzzy PID control system. Current approaches frequently depend on energy-intensive embedded digital systems, consuming substantial energy levels ranging from a few μW to mW. To address this limitation we propose a fully analog design offering insights into the potential of analog circuits for power-efficient robust control in complex and uncertain environments. It consists of Gaussian function, min/max, Operational transcoductance amplifier circuits and Resistor-Capacitor networks for the implementation of the fractional-order components. Crafted for operation under a reduced voltage supply (0.6 V), the controller attains minimal power usage (861.8 nW), facilitating uninterrupted, extended-term functioning. Post-layout simulation results confirm the proper operation of the proposed design. The proposed system is designed and simulated using the Cadence IC Suite in a TSMC 90 nm CMOS process.

Keywords: PID controller; analog integrated; low-power design; type-2 fuzzy controller

Citation: Alimisis, V.; Eleftheriou, N.P.; Georgakilas, E.; Dimas, C.; Uzunoglu, N.; Sotiriadis, P.P. A Low Power Analog Integrated Fractional Order Type-2 Fuzzy PID Controller. *Fractal Fract.* **2024**, *8*, 234. https://doi.org/10.3390/fractalfract8040234

Academic Editors: António Lopes, Carlo Cattani, Kang-Jia Wang and Inés Tejado

Received: 15 January 2024
Revised: 25 March 2024
Accepted: 12 April 2024
Published: 16 April 2024

1. Introduction

In the realm of control systems, the evolution from conventional crisp logic to more nuanced methodologies has paved the way for advanced control strategies. One such paradigm, fuzzy logic, has garnered substantial attention for its capacity to emulate human-like decision-making processes [1,2] and effectively handle complex and uncertain environments [3]. Fuzzy logic, introduced by Lotfi A. Zadeh in the 1960s [4], models imprecision and uncertainty through linguistic variables and membership functions (MFs), offering a bridge between the quantitative precision of digital systems and the qualitative reasoning of human cognition [5].

Fuzzy Set Theory presents essential mathematical instruments for executing numerical computations grounded in linguistic descriptions and mathematically defined concepts through membership functions as fuzzy sets [6,7]. A fuzzy set denotes a group of entities exhibiting varying degrees of membership [8]. This set is defined by an MF assigning a membership grade from zero to one to each entity [9], denoting the entity's connection strength to the fuzzy set. Moreover, within Fuzzy Inference Systems (FIS), pivotal components for simulating human expertise and knowledge encompass fuzzy if-then rules [6,7]. The amalgamation of Fuzzy Inference Systems with Neural Networks (NNs) and Machine Learning (ML) optimizations leads to the emergence of a groundbreaking field known as Neuro-Fuzzy Computing (NFC), the core of intelligent soft computing systems [10].

A significant offshoot of fuzzy logic's applications is its integration into Proportional-Integral-Derivative (PID) controllers, giving rise to the realm of fuzzy PID control [11]. The conventional PID controllers, known for their simplicity and effectiveness, have now been augmented with fuzzy logic's ability to handle non-linearity and uncertainty [3]. The synergy of these concepts has led to the development of type-2 fuzzy PID controllers,

wherein the inherent uncertainties are not only considered but also managed effectively, enhancing control in intricate systems [12,13].

In assessing the merits of fuzzy PID control over its conventional counterpart, noteworthy advantages emerge [14]. Fuzzy PID controllers inherently encapsulate imprecision, enabling them to robustly handle complex systems characterized by vague, uncertain, or even contradictory information [15]. When evaluating the superiority of fuzzy PID control compared to its traditional counterpart, several significant benefits become apparent. Fuzzy PID controllers possess an innate capacity to accommodate imprecision, which equips them to adeptly navigate intricate systems marked by vague, uncertain, or conflicting information. This inherent adaptability enables fuzzy PID controllers to robustly address challenges that conventional PID controllers might struggle with [15]. However, it's important to acknowledge that the utilization of linguistic rules and membership functions (MFs) within fuzzy PID controllers can introduce a layer of intricacy into the design process. Designers are thus required to possess a thorough comprehension of the system's dynamics and behavior to effectively implement fuzzy PID control strategies [15]. On the flip side, the reliance on linguistic rules and MFs might introduce a level of complexity in the design process, necessitating a comprehensive understanding of the system's behavior [14]. Despite this potential complexity, the flexibility and resilience afforded by fuzzy PID controllers make them a compelling choice for managing complex systems in various domains. Moreover, their ability to gracefully handle uncertainty and imprecision renders them particularly suitable for applications where precise modeling is difficult or impractical, ultimately leading to enhanced performance and robustness in real-world scenarios [14].

As technology forges ahead, the choice of implementation platform becomes increasingly versatile. Analog circuitry emerges as a compelling alternative to digital platforms like embedded systems, Field-Programmable Gate Arrays (FPGAs), and microcontrollers [16]. The analog approach, explored in this paper, can harness the intrinsic parallelism of electrical signals to achieve real-time computation and control, promising potential advantages in terms of low-power consumption, reduced latency, and area efficiency. However, this avenue comes with its own set of challenges, such as susceptibility to noise and limited scalability. Applications of fuzzy controllers span various domains, including industrial automation [17], automotive control [18], and biomedical systems [19], where real-time processing, power efficiency, and reliability are paramount.

The goal of the current work is to propose a low-power hardware purely analogue implementation of a system combining fractional calculus with the advantages fuzzy logic. The main purpose is to implement the selected control method on hardware with the proposed architecture and compare with software/Matlab implementation as a proof of concept. The comparison with other control types should be issued by other works focusing on the mathematical structures and modelling of the various control approaches. Within the existing literature are reported such implementations varying from fractional order (FO) filters to fractional 'LC' resonators. In [20] a FO filter based on current and voltage conveyors operating as active elements is proposed. It is implemented on the TSMC 0.18 µm CMOS process occupying 0.0015 mm^2 of silicon area with 380.6 µW power consumption. In [21] FO low-pass and high-pass filters based on operational transconductance amplifiers (OTAs) are exhibited. They are designed on the TSMC 0.35 µm CMOS process and consume power up to 47.5 nW depending on the order and type of the filter. In [22] FO Chaotic Systems are realized using active filters based on OTAs. They are designed on the UMC 180 nm CMOS node and only one OTA consume power varying between 36 µW and 540 µW. FO differentiators and integrators with low unity-gain frequency of 100 kHz are presented in [23], while a tunable FO resonator is proposed in [24]. The last two works are implemented on AMS 0.35 µm CMOS technology. Relying on the need for low-power systems, here a low-power control system is proposed. The major contributions of this work are:

- The low-power performance, operating in subthreshold regime.

- The pure analog implementation of a PID controller that combines both Fuzzy logic and fractional calculus to control the plant system.

The remainder of this paper is organized as follows. Section 2 delves into the theoretical underpinnings of type-2 fuzzy PID control. In Section 3 we expound upon the architecture of the proposed analog controller, elaborating on the main building blocks of it in Section 4. Section 5 presents simulation results, and juxtaposes the analog approach against software implementations for a 2nd order stable linear plant along with dead time. Lastly, in Section 6, conclusive comments are provided that encapsulate the study's discoveries.

2. Background

Fractional-order fuzzy controllers represent a cutting-edge paradigm in control system theory, amalgamating the robustness of fractional calculus with the adaptive reasoning of fuzzy logic [25]. These controllers epitomize a sophisticated fusion of mathematical precision and cognitive flexibility, ushering in a new era of control strategy refinement [26]. By embracing fractional calculus, they adeptly handle complex, non-integer dynamics, capturing intricate system behaviors that traditional integer-order controllers struggle to characterize [27]. Moreover, leveraging the innate adaptability of fuzzy logic, these controllers excel in navigating ambiguous and uncertain environments, employing linguistic variables and membership functions to interpret imprecise data and make informed control decisions [28]. This amalgamation offers a versatile toolkit for handling intricate control problems where conventional approaches fall short, enabling nuanced and adaptive control in dynamic, real-world systems.

2.1. Literature Review

The evolution of fuzzy controllers, extensively documented in a vast and diverse literature, stems from Lotfi Zadeh's seminal contributions in the 1960s [4]. Zadeh's groundbreaking conceptualization of fuzzy sets and logic laid the early theoretical groundwork, reshaping how control systems handle imprecise data [4,29]. This foundational phase delved into the exploration of membership functions, fuzzy rules, and inference mechanisms, laying the cornerstone for managing uncertainties in decision-making processes within control systems [30].

As the field progressed, the literature expanded its horizons, illustrating a myriad of practical applications spanning industries. In the realm of industrial automation, fuzzy controllers found homes in an array of settings, from optimizing power systems [31–33] and managing traffic flow [34–36] to orchestrating robotic operations [37–39]. These real-world implementations demonstrated the adaptability and effectiveness of fuzzy logic in scenarios where traditional mathematical models struggled due to system complexity and unpredictable variables. Notably, within manufacturing and automotive engineering, the success stories abound, showcasing how fuzzy controllers optimize production processes and seamlessly integrate into vehicle control systems, including the critical functionality of anti-lock braking systems [40,41].

The chronicles of fuzzy control methodologies reveal a rich tapestry of advancements chronicled in the literature. Hybrid systems emerged as a prominent theme, spotlighting the fusion of fuzzy logic with other control paradigms like neural networks [42–44] or genetic algorithms [45–47]. These hybrid models leverage the complementary strengths of different methodologies, bolstering system performance, resilience, and adaptability across various applications. The ever-expanding literature on fuzzy controllers dynamically responds to emerging challenges and frontiers. Recent research has shifted focus towards explainable AI, seeking to render fuzzy controllers more transparent and interpretable. This thrust aligns with the imperative for ethical and accountable AI systems, particularly in critical domains where the rationale behind decisions holds paramount importance. In summation, the literature landscape surrounding fuzzy controllers offers an expansive panorama that not only elucidates the theoretical underpinnings and practical applications but also navigates

the evolving terrains of interdisciplinary collaborations, technological innovations, and ethical considerations within the domain of control systems and artificial intelligence.

In recent years, there has been a growing interest in the analogue implementation of fractional-order controllers, driven by their potential in enhancing the performance and adaptability of control systems. In [48] is explored the integrated technology for fractional-order proportional-integral-derivative (PID) design, providing insights into the practical realization of such controllers in engineering applications. Ref. [49] focused on the efficient analog implementations of fractional-order controllers. The work [50] contributes to the field by developing fractional-order analog integrated controllers, offering application examples that demonstrate the versatility of these implementations. In [51] new alternatives for analog implementation of fractional-order integrators, differentiators, and PID controllers are presented, highlighting the use of integer-order integrators in the realization process. Additionally, the presented work in [52,53] laid the foundation for analogue realizations of fractional-order controllers, exploring their applications in temperature control and motor control. Further contributions from [54] investigated the fractional-order feedback control of a DC motor, while [55] delved into CMOS fuzzy logic controllers supporting fractional polynomial membership functions. This body of literature collectively underscores the advancements and diverse applications of analogue fractional-order controllers in various engineering domains.

2.2. Fractional PID Control

A classic integral-order PID controller consists of three responses: proportional, integral and derivative [56,57]. There are other controllers such as PD, PI, ID, and P controllers, but in this work, we focus on designing PID controllers [56]. The response $u(t)$ of a PID controller is the sum of the three aforementioned responses [56] and the equation is as follows:

$$u(t) = K_p \cdot e(t) + K_i \cdot \int_0^t e(\tau)d\tau + K_d \frac{de(t)}{dt} \tag{1}$$

where $e(t) = r(t) - y(t)$ is the error between the output $y(t)$ of the system and the reference input $r(t)$ that the output should follow. The first term in the above equation corresponds to the proportional (P) part of the controller, the second to the integral (I) and the third to the derivative (D). Applying the Laplace transform to Equation (1) in order to obtain the frequency domain response results in:

$$U(s) = K_p \cdot E(s) + K_i \frac{E(s)}{s} + K_d \cdot sE(s) \tag{2}$$

where $E(s)$ is the output error in the frequency domain. Dividing by $E(s)$ results in the transfer function of the integral order PID controller

$$G(s; K_p, K_i, K_d) \equiv \frac{U(s)}{E(s)} = K_p + \frac{K_i}{s} + K_d \cdot s \tag{3}$$

However, PID controllers face difficulties in the presence of non-linearities/non-idealities due to their inherent linearity [58,59]. Besides, in recent years, fractional calculus has found applications in the modeling and control of diverse physical systems, as analyzed explicitly in Section 2.1. Therefore, to effectively account for the above disadvantages, the idea of fractional order PID (FO-PID) controllers was conceived; the FO-PID controller is the result of extending the conventional PID controller based on fractional calculus [58,59]. In the FO-PID controller, in addition to the proportional, integral, and derivative parameters (K_p, K_i, and K_d) two additional parameters are present: the order of fractional integration λ and the order of fractional differentiation μ, with $0 < \lambda, \mu < 1$ [60]. An FO-PID controller is denoted as $PI^{\lambda}D^{\mu}$, where λ and μ the parameters mentioned above. Having five parameters offers extra flexibility to the controller. Fractional calculus allows the differential and integral terms to be of arbitrary order, not necessarily integers.

Similarly to the conventional PID controller, the time response of FO-PID controller is

$$u(t) = K_p \cdot e(t) + K_i \cdot D^{-\lambda} e(t) + K_d \cdot D^{\mu} e(t) \tag{4}$$

where $D^{-\lambda}$ denotes the fractional integration operator of order λ and D^{μ} the fractional differentiation operator of order μ. Applying the fractional Laplace transform yields the transfer function of the FO-PID controller in the frequency domain

$$G(s; K_p, K_i, K_d, \lambda, \mu) \equiv \frac{U(s)}{E(s)} = K_p + \frac{K_i}{s^{\lambda}} + K_d \cdot s^{\mu} \tag{5}$$

As observed, $\lambda = 1$ and $\mu = 1$ corresponds to an integral order PID. Similarly, $\lambda = 0$ and $\mu = 1$ is a PD controller, $\lambda = 1$ and $\mu = 0$ is a PI controller and $\lambda = 0$ and $\mu = 0$ is a P controller. Various values of λ and μ within the interval (0,1), results in an FO-PID, showcasing the distinct flexibility and enhanced precision of this controller. It allows for better adaptation of the dynamic properties of a system, providing the capability for improved adjustment.

2.3. Type-2 Fuzzy PID Control

Fuzzy logic, an extension of traditional binary logic, addresses the inherent ambiguity in real-world data by introducing the concept of fuzzy sets. A fuzzy set represents the membership of elements within a given set with degrees ranging between 0 and 1. The MF, denoted as $\mu_A(x)$, quantifies the extent to which an element x belongs to the fuzzy set A [4,61].

Fuzzy PID controllers offer a robust and adaptable solution for controlling complex systems characterized by nonlinearities and uncertainties. By integrating fuzzy logic with the classic PID algorithm, these controllers can effectively handle varying operating conditions, providing stable and precise control. Their ability to dynamically adjust control parameters based on linguistic rules enables smoother setpoint tracking, enhanced disturbance rejection, and reduced tuning efforts. Fuzzy PID controllers find application across diverse industries, offering versatility and ease of implementation while delivering reliable performance in challenging control scenarios. Overall, their combination of robustness, adaptability, and ease of use makes them a valuable tool for engineers seeking efficient control solutions for a wide range of systems and applications.

Fuzzy reasoning applies this concept to decision-making, enabling systems to handle imprecise data effectively [3]. This reasoning operates through a collection of fuzzy rules, which are typically presented in IF-THEN format, where the "IF" part refers to the conditions or states of the system (*antecedents*), and the "THEN" part dictates the corresponding action (*consequents*) [61]. Fuzzy inference systems comprise rules that connect linguistic variables through linguistic expressions, offering a means to model human-like thinking processes [1,2]. The aggregation and combination of multiple fuzzy rules are integral to the fuzzy inference process. Different fuzzy rules might contribute to the control decision, and their effects need to be synthesized into a coherent control action. This involves the utilization of operators such as "AND", "OR", and "NOT" to manage the combination of membership degrees associated with linguistic terms. The "AND" operator, for example, captures the intersection of different linguistic terms, allowing for the expression of more complex conditions. The "OR" operator, on the other hand, models the union of these terms, enabling the control system to react to a broader range of conditions [61]. Type-2 Fuzzy Inference Systems (FIS), particularly Type-2 Mamdani FIS, extend this by considering uncertainties in both input and output variables. In such systems, MFs for the linguistic terms themselves become fuzzy sets, allowing for a more robust representation of uncertainty [62].

Fuzzy control employs fuzzy logic to create control strategies that adapt to dynamic and uncertain environments. This methodology comprises three main components: fuzzification, inference, and defuzzification. Fuzzification translates crisp inputs into linguistic variables characterized by MFs. The inference process involves applying a set of fuzzy

rules, to determine control actions. The Type-2 Mamdani FIS, as an example, handles uncertainties by assigning intervals to membership degrees. The defuzzification step maps fuzzy control outputs back into crisp control signals [12].

Within the framework of fuzzy PID control, the traditional Proportional-Integral-Derivative (PID) controller gains remain constant. However, the approach diverges by employing fuzzy reasoning to modify the controller's output, as illustrated in Figure 1. Specifically, the controller receives two inputs; the error $e(t)$ and its derivative $\frac{de(t)}{dt}$ and scales them to accomodate to the fuzzy MFs' domain. These inputs are subjected to fuzzy reasoning within the Type-2 Mamdani FIS which generates an output $u(t)$ that adjusts the control signal. The altered $u(t)$ is subsequently rescaled and integrated before being fed as input to the plant [13,63,64].

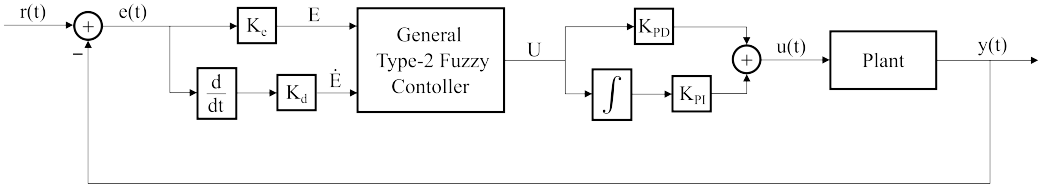

Figure 1. Integral order PID general type-2 fuzzy logic system structure.

3. Proposed Design Methodology

In this section, the high level architecture of the proposed analog Fuzzy Fractional Order PID controller is presented. In Section 2 the concepts of fuzzy logic controllers and conventional logic integral order controllers were analyzed. Combining the above two types of control systems, leads to the Fractional Order Fuzzy PID (FO-FPID) controllers [25,65], that benefit from the advantages of both the extra parameters of fractional controllers and the flexibility of fuzzy logic to describe physical systems with inherent non-idealities.

The structure of the proposed analog FO-FPID controller is illustrated in Figure 2. The input $v_e(t)$ corresponds to the error $e(t)$ between the system output and the reference input scaled to the voltage domains of the circuit. The two single-input single-output amplifiers provide the required gains K_E and K_{CE} to scale the signal prior to the Fuzzy Inference System, while the other two amplifiers provide the control gains K_{PD} and K_{PI}, that are tuned in order to achieve the desired performance for the plant. The Constant Phase Elements (CPEs), explained in Section 4.1, are able to operate as fractional order derivation and integration circuits [66]. The order of the fractional operation, μ for derivation and λ for integration, as well as the kind of operation are tuned through the components comprising each CPE. The core of the controller is the Fuzzy Inference System (FIS) that consists of the fuzzification block, the fuzzy reasoning system that deals with the rules and the defuzzification circuit that utilizes the Center Of Gravity (COG) method to provide the crisp output. The aforementioned blocks are analyzed in Sections 4.1–4.4. Furthermore, voltage-to-current (V/I) and current-to-voltage (I/V) converters are used so as to perform the addition of the two terms at the output of the controller and subsequently convert again this signal to the output voltage of the controller $v_u(t)$. This signal is the voltage that is fed as input to the plant system to control its response.

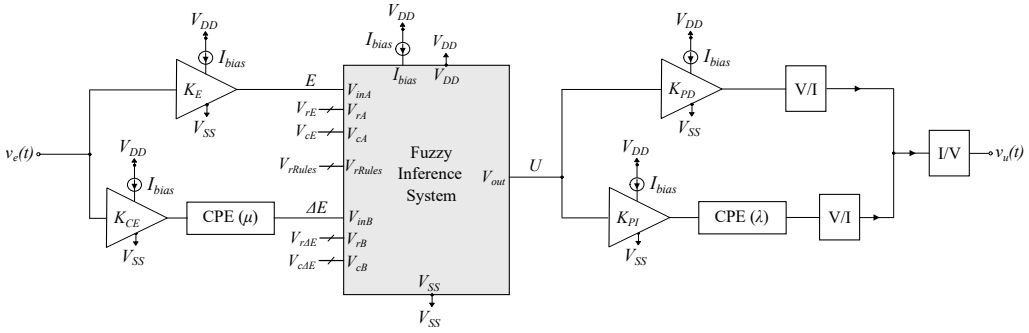

Figure 2. The proposed architecture of the Fractional Order Fuzzy PID controller. The input corresponds to the error $e(t)$ between the system output and the reference input scaled in the voltage domains of the circuit, while the output is the voltage that is fed as input to the plant.

4. Circuit Implementation

4.1. Fractional Order Circuits

Integrators and differentiators play a pivotal role as building components for the realization of filters, oscillators, control systems and more. The literature has already featured published works on fractional-order digital implementations of these circuits [67,68]. Currently, there are no commercially available devices for the physical implementation of fractional-order circuits and systems. Consequently, classic integral-order devices are used utilizing approximations, like Continued Fraction Expansions (CFEs) [69,70] as well as rational approximation methods [71,72], to achieve the desired performance. A substantial research endeavor is underway to advance the development of fractional-order capacitors, commonly referred to as Constant Phase Elements (CPEs), functioning as independent two-terminal devices and realizing the transfer function

$$H(s) = ks^a \tag{6}$$

where k is a constant and a denotes the order of the fractional operation [73].

Current methodologies for emulating a CPE predominantly depend on passive RC trees. The components of these trees can be derived through various techniques, including the continued fraction expansion method. Adhering to this methodology, numerous fractional-order circuits have been documented in the literature, employing diverse RC network topologies [74–78]. In this work, for the required fractional-order elements, that implement the fractional derivative and integral, the 5th order Cauer I form [73], is selected after simulating among various forms and addressing for the accuracy of the approximation along with their simplicity.

The expression for the impedance of this two-terminal network is

$$Z(s) = R_1 + \frac{1}{C_1 s + \frac{1}{R_2 + \cdots \frac{1}{R_n + \frac{1}{C_n s + \frac{1}{R_o}}}}} \tag{7}$$

where n is the order of the approximation. The Cauer I n^{th}-order approximation used for a CPE is illustrated in Figure 3. The values of R-C elements are summarized in Table 1.

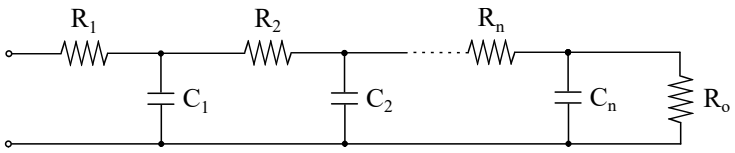

Figure 3. The Cauer I form for approximating a CPE via CFE.

Table 1. Cauer I form R-C values.

Resistors	R (kΩ)	Capacitors	C (pF)
R_0	833.6	-	-
R_1	696.3	C_1	20
R_2	561.6	C_2	137.2
R_3	504.6	C_3	428.7
R_4	496.5	C_4	1069.3
R_5	545.2	C_5	2835.6

4.2. Gaussian Function Circuit

The fuzzification module serves as a critical intermediary between the Fuzzy Inference System (FIS) and the external environment, typically interfacing with sensors that deliver signals in voltage mode. Additionally, this module interacts with the fuzzy inference block (FI), particularly utilizing the min-max operator. In this context, a Bump circuit functions as the fuzzification block. While numerous Bump circuits have been developed across various applications, for the purposes of this investigation, a customized version of the Bump circuit (with an aspect ratio of 7) has been chosen to enhance the quality of the Gaussian curve. This modified circuit, as depicted in Figure 4 and detailed in [79], facilitates an improved Gaussian curve generation. Specifically, the circuit incorporates a symmetric current correlator (comprising transistors $M_{p1} - M_{p6}$ in Figure 4) to ensure symmetry around the mean value, even with minute currents [80]. The output current I_{out} of the Gaussian circuit is illustrated in Figure 5. Moreover, by setting the ratio to 7, an expansion of the circuit's linear region is achieved, resulting in higher variance for the same V_c. To further enhance mirroring performance, especially with low bias currents, a cascode current mirror including transistors $M_{n5} - M_{n10}$ (Figure 4) has been integrated. The mean value of the Gaussian curve is determined by the voltage V_r, while the variance and height are regulated by the voltages V_c and the bias current I_{bias}, respectively. The dimensions of the transistors used in the circuit are summarized in Table 2.

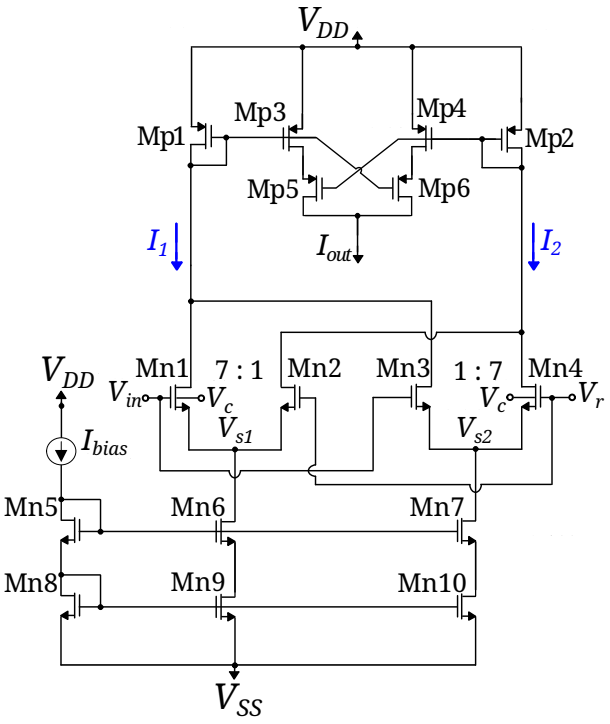

Figure 4. The employed Bump circuit is shown. The resultant output current, denoted as I_{out}, mirrors a Gaussian function modulated by the input voltage V_{in}. The voltage parameters V_r, V_c, and the bias current I_{bias} adjust the mean value, variance, and peak value of the Gaussian function, respectively.

Table 2. Bump Circuit Transistors' Dimensions.

NMOS Differential Block	W/L (µm/µm)	Current Correlator	W/L (µm/µm)
M_{n1},M_{n4}	2.8/0.4	M_{p1},M_{p2}	1.6/1.6
M_{n2},M_{n3}	0.4/0.4	M_{p3},M_{p4}	0.4/1.6
M_{n5}–M_{n8}	0.4/1.6	M_{p5},M_{p6}	0.4/1.6
M_{n9},M_{n10}	1.6/1.6	-	-

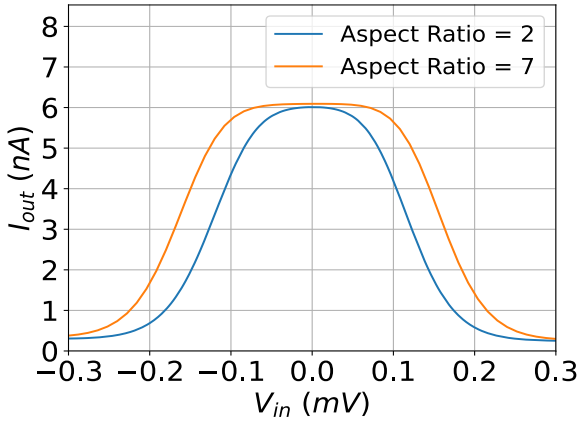

Figure 5. The output current of the applied Gaussian function circuit is analyzed with regard to the sizing of the input differential pair transistors. The simulation was carried out with V_r set to 0 V, V_c at 180 mV, and I_{bias} at 6 nA.

To understand the high-level structure of the Fuzzification subsystem within the utilized FIS, let's consider V_{in1} as the input to the system, representing the fuzzy variable A. This variable is characterized by n linguistic terms, denoted as A_1 to A_n. These terms correspond to a fuzzy set characterized by a Gaussian Membership Function (MF), defined at the system level by its respective FMF circuit and biasing parameters. As mentioned earlier, the output current I_{FMF} from each FMF circuit signifies the membership grade or the degree of compatibility between the input V_{in1} and the specific fuzzy set it represents. The high-level structure of the Fuzzification block in the FIS is depicted in Figure 6.

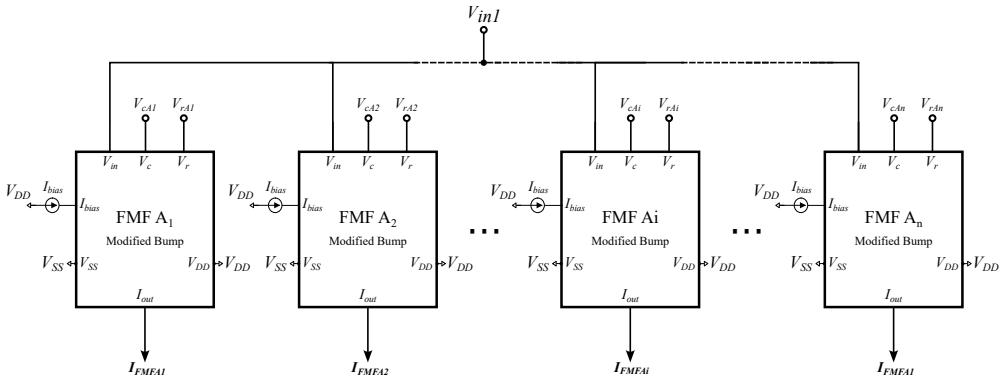

Figure 6. The Fuzzification block within the FIS exhibits a high-level architecture where each FMF_{Ai} circuit corresponds to a specific linguistic term, A_i, associated with the linguistic variable A. The bias current I_{bias} remains a constant across all FMF circuits, set at 3 nA in our case. Meanwhile, the voltages V_r and V_c are variable, ranging from −300 mV to +300 mV. The resulting output current I_{FMF} signifies the degree of compatibility existing between the input V_{in} of the FMF and the particular fuzzy set it represents.

4.3. MIN/MAX Circuit

The MIN/MAX operators are widely used in a variety of applications within nonlinear signal processing tasks or control theory. Various methods have been suggested in the literature, encompassing Winner-Take-All or Loser-Take-All circuits alongside comparators, related to Fuzzy theory [81,82]. The implemented design of the MIN/MAX operator, as proposed in [83] opts for systems with only two inputs. However, it can also handle rules with multiple antecedents, by connecting these cells in cascaded format. Although this approach does not prioritize area and power efficiency, it facilitates intricate fuzzy logic with rules combining AND-ed and OR-ed antecedents.

Additionally, the design employed in this architecture executes all operations concurrently, circumventing the drawbacks of high chip (area) usage and energy consumption linked to employing distinct designs for MAX and MIN operations. Given the absence of multi-input circuits integrating these two operations, the requirement for two separate blocks becomes necessary otherwise. The Fuzzy Inference (FI) circuit utilized to determine the firing strength of the implemented FIS rules is founded on a pioneering current-mode max-min design [84], depicted in Figure 7.

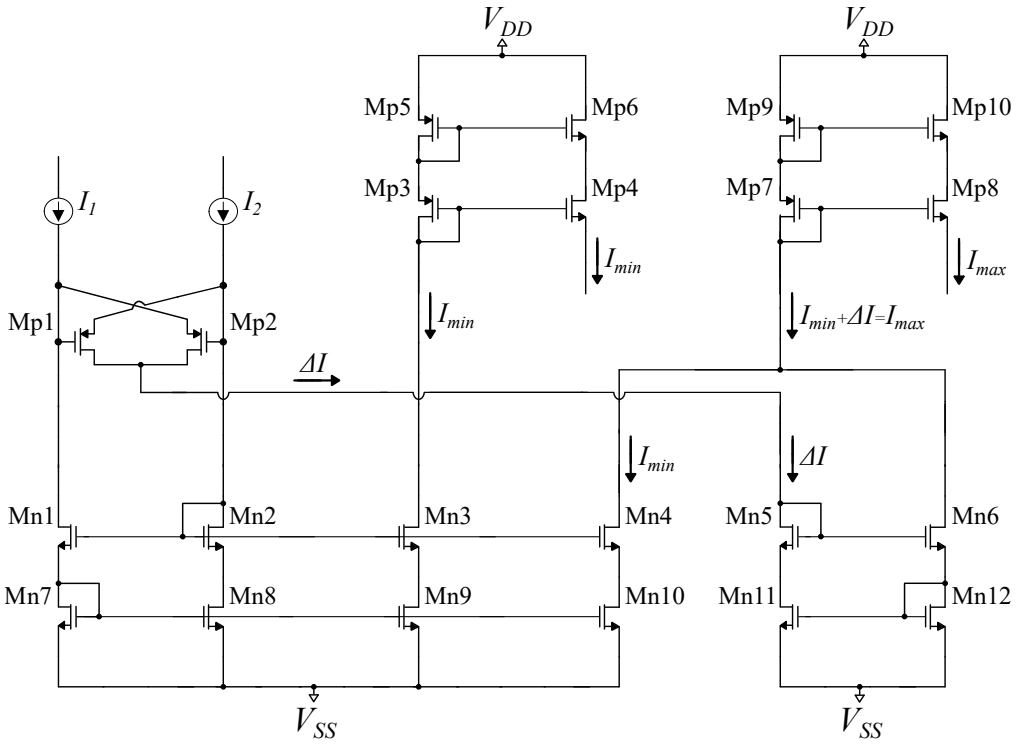

Figure 7. The implementation of the Min/Max circuit. It provides both operations.

Given that the input parameters (currents) within the design are expected to be small, on the order of nA, larger elements are incorporated to bolster the design's efficacy. However, augmenting the length consequently escalates the output impedance while concurrently reducing the input impedance. Conversely, diminishing the width contributes to heightened precision in mirroring small currents. The dimensions of the transistors are equal to $\frac{W}{L} = \frac{0.2\mu m}{1.6\mu m}$. In Figures 8 and 9 the transient outcomes of the FI circuit within the implemented architecture showcase two currents in sinus format, each with an magnitude of 10 nA and a phase delay of one hundred ten deg.

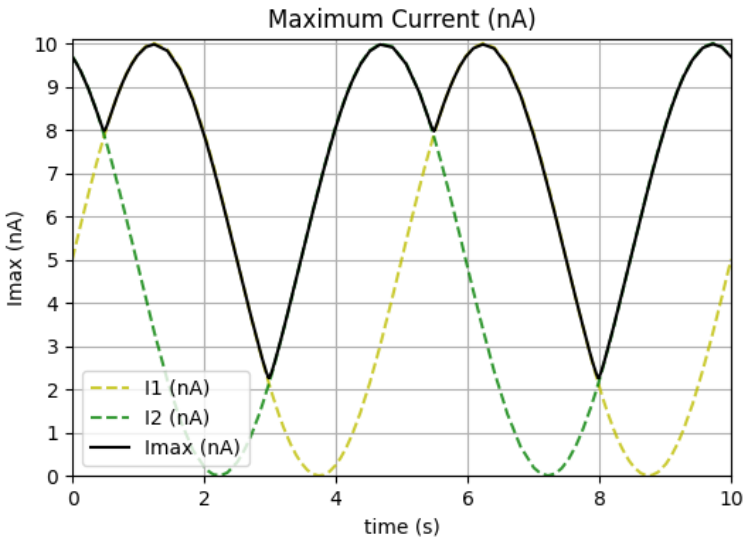

Figure 8. Maximum output current of the FI circuit for two input sinusoidal current waveforms with 10 nA amplitude and a phase shift of 110 deg.

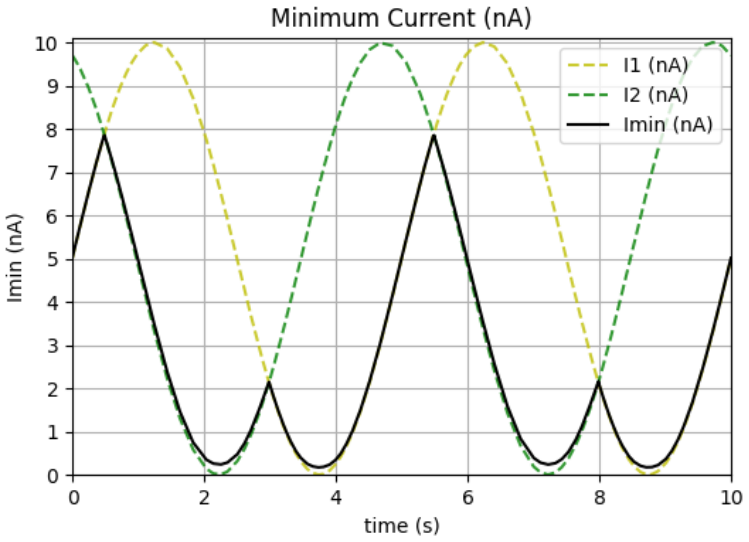

Figure 9. Minimum output current of the FI circuit for two input sinusoidal current waveforms with 10 nA amplitude and a phase shift of 110 deg.

Within the implemented FIS, each FI block embodies a specific fuzzy rule by employing a series of FI circuits to amalgamate multiple antecedents. Each individual FI circuit integrates a fuzzy rule comprising two antecedents. The output current of the FI circuit is purposefully chosen as either the MIN or MAX current, culminating in either ANDed or ORed antecedents, respectively.

4.4. COG Circuit

Following the mathematical framework, and considering that the firing strength ω_i of $Rule_i$ equates to the output current $I_{FIRulei}$ of the i-th FI block, while the centroid of the consequent Gaussian membership function (MF) of the same rule corresponds to the voltage setting V_{rRulei}, the determination of the center of gravity (COG) for the comprehensive output MF of the envisioned Fuzzy Inference System (FIS) comprising m rules is expressed as follows:

$$COG = \frac{\sum_{i=1}^{m} I_{FIRulei} \cdot V_{rRulei}}{\sum_{i=1}^{m} I_{FIRulei}}. \quad (8)$$

Among the array of analog COG defuzzification strategies documented in the literature [85,86], the implemented design incorporates a voltage follower-aggregation method initially introduced by Carver Mead in [83,87]. This technique, depicted in Figure 10, serves as the foundational architecture.

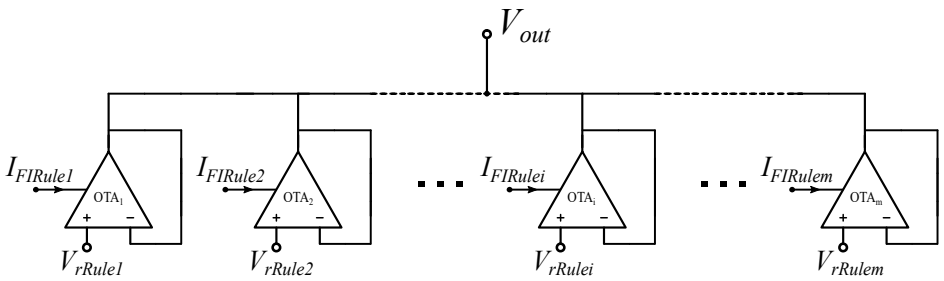

Figure 10. The high-level architecture of the Defuzzification block within the FIS comprises a follower aggregation circuit. This circuit is pivotal in the system's operation, leveraging a follower-aggregation technique to determine the output's center of gravity. This technique, derived from Carver Mead's work, forms the core of the system's defuzzification strategy, ensuring accurate and efficient computation of the final output from the fuzzy logic inference process.

Utilizing a collective of m Operational Transconductance Amplifiers (OTAs), denoted as OTA_1 to OTA_m, the system aggregates the weighted inputs V_{rRule1} through V_{rRulem} while computing the weighted average outlined in Equation (8) across each dimension of the system's output vector [83]. This operation hinges on the feedback loop illustrated in Figure 10 and adheres to Kirchhoff's current law to attain:

$$\sum_{i=1}^{m} G_{mi} \cdot (V_{rRulei} - V_{out}) = 0 \quad (9)$$

The transconductance G_{mi} pertaining to the operational mode of OTA_i, while it operates within its linear range, is expressed as:

$$G_{mi} = \frac{I_{FIRulei}}{2kT/(q\kappa)}. \quad (10)$$

In this context, $I_{FIRulei}$ stands as the bias current specific to OTA_i.

For the range of input values that the OTA circuits are adjusted to operate in their linear region with transconductance described from Equation (10) and supposing that the OTAs in the OTA-bank of Figure 10 are matched, the evaluation of Equation (9) leads to the desired result of Equation (8) as output of the follower-aggregation structure. Due to the fact that both the aggregation and the defuzzification processes require only one tuning voltage parameter V_r for each consequent membership function, this implementation aligns with the implemented FIS. This simplicity arises from the OTAs' biasing currents, which are generated by the FI subsystem.

Hence, the necessity for voltage to current and current to voltage converters, as well as extensive area multiplier/divider circuits, is circumvented. This avoidance streamlines the system's architecture significantly. For accuracy assurance within the block, a wide-range high open loop gain OTA has been specifically designed [83]. Figure 11 depicts this OTA, ensuring the fidelity and precision crucial for the system's performance.

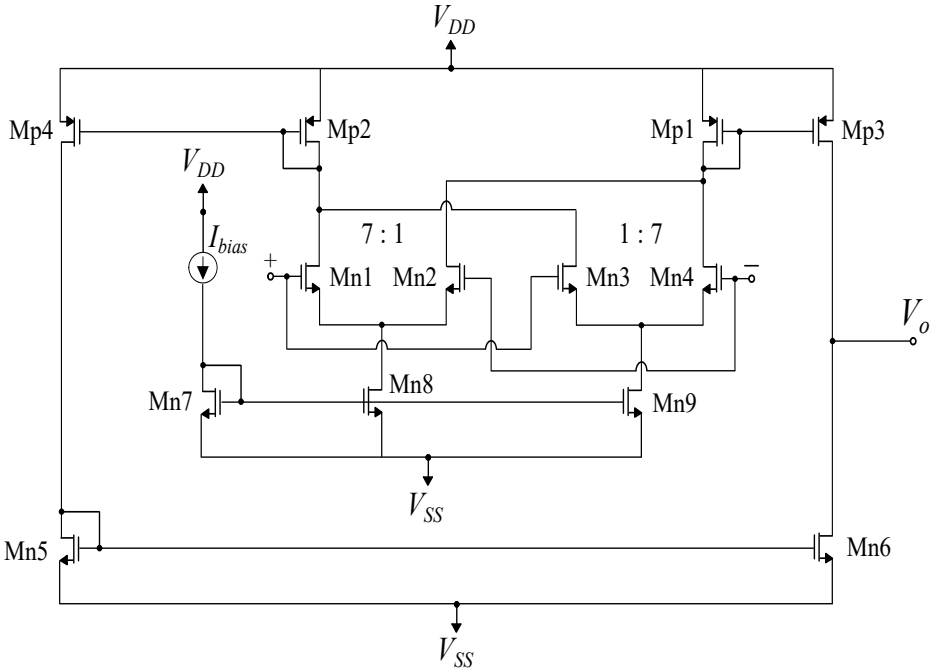

Figure 11. Wide Range Cross Coupled Operational Transcoductance Amplifier.

The cross-coupled differential pair composed of transistors M_{n1}–M_{n4}, designed with a ratio of 7, operates alongside current mirrors M_{p2}, M_{p4}, M_{p1}, M_{p3}, M_{n5}, and M_{n6}, effectively addressing the inherent V_{min} issue in conventional OTAs as described in [87]. This configuration substantially expands the linear operating region of the OTA, enhancing its performance. The elongated transistors M_{p3} and M_{n6} intentionally induce low drain conductance, thereby endowing the circuit with heightened open-loop voltage gain and output impedance characteristics. These deliberate design choices optimize the OTA's functionality and stability. For detailed specifications, the dimensions of all transistors utilized in this design are outlined in Table 3.

Table 3. Dimensions of transistors (Figure 11).

Differential Pair	W/L (μm/μm)	Current Mirrors	W/L (μm/μm)
M_{n1}, M_{n4}	1.4/16.0	M_{p1}, M_{p3}	1.8/16.0
M_{n2}, M_{n3}	0.2/16.0	M_{p2}, M_{p4}	0.8/16.0
M_{n7}	0.2/16.0	M_{n5}, M_{n6}	0.2/16.0
M_{n8}, M_{n9}	0.2/16.0	-	-

The rule base contains a set of fuzzy rules defining the relationships between input and output linguistic variables. Through the process of fuzzy inference, input values are evaluated against these rules to determine the appropriate output values, thereby shaping the control surface that governs the system's behavior. The control surface of a fuzzy inference controller graphically interprets the mapping between input linguistic variables and output linguistic variables. For the designed controller the fuzzy system's surface is depicted in Figure 12.

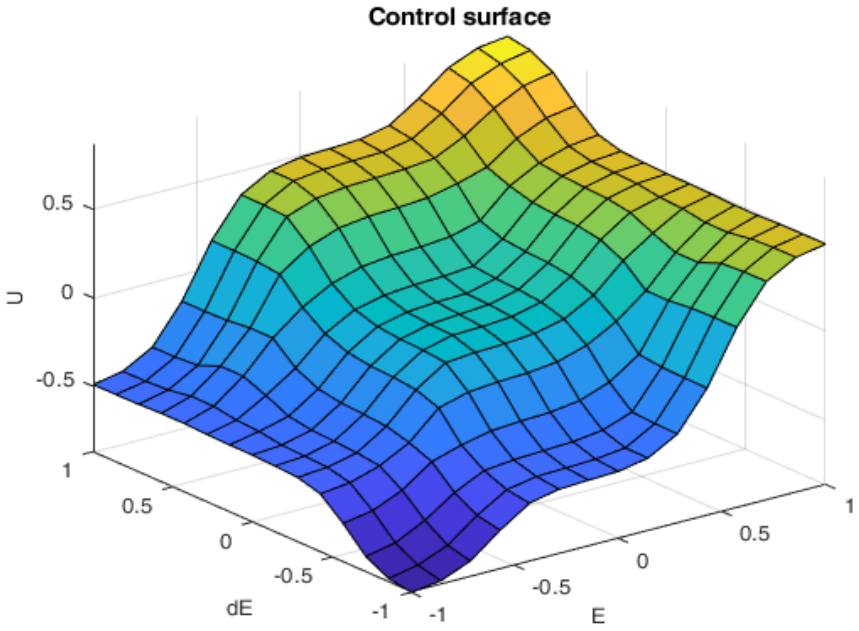

Figure 12. The control surface of the implemented fuzzy inference controller.

5. Application Example and Simulation Results

In this study, the efficacy of the proposed FO-FPID controller is thoroughly evaluated through extensive Matlab simulations on a carefully selected plant model. We opted for a first-order nonlinear system with dead time due to its significance and relevance in real-world processes, making it a representative testbench for control strategies:

$$\dot{y}(t) = y(t) + \sin^2\left(\sqrt{|y(t)|}\right) + u(t - L) \tag{11}$$

where $u(t), y(t)$ are the system's input and output respectively and the parameter L represents dead time. The reference input $r(t)$ that the system should follow is a step function. Moreover an external perturbation is added to the system at $t = 10$ s to test the controller's ability to compensate this disturbance keeping the system at the required state.

The advantages of our chosen plant lie in its ability to emulate complex and realistic behaviors encountered in processes such as chemical reactors, mechanical systems, and biological systems [88]. The presence of nonlinearity and dead time introduces challenges that controllers must overcome, reflecting the robustness and adaptability required for practical control applications. By employing this particular plant, our simulations aim to showcase the controller's performance under conditions that mirror the intricacies of dynamic systems found in diverse fields, thereby enhancing the generalized ability and applicability of the proposed FO-FPID control strategy. A comprehensive comparison is undertaken by benchmarking the analog integrated FO-FPID controller against the software-based one.

In [11,89] the chosen controllers are likely to represent a diverse range of control strategies, each with its unique strengths and limitations. This selection may include classic controllers such as PID, as well as more advanced controllers like Model Predictive Control (MPC), Sliding Mode Control (SMC), or Adaptive Control algorithms. The inclusion of these diverse control strategies allows for a thorough assessment of the FO-FPID controller's performance under various operating conditions and system dynamics. The comparison involves evaluating the response of each controller concerning Key Performance Indicators (KPIs). Metrics such as rise time, overshoot, settling time, steady-state error, and robustness to disturbances are considered. These metrics provide quantitative

insights into the controllers' abilities to achieve desired setpoints, respond to changes in the system, and maintain stability in the presence of uncertainties. Furthermore, simulations are conducted to analyze the controllers' transient and steady-state behaviors. The responses to step changes, input disturbances, and external perturbations are observed to assess the controllers' robustness and adaptability to different operating scenarios.

Software-based refers to the implementation of the closed-loop system (both plant and controller) in the environment of Matlab/Simulink using Fuzzy Logic Toolbox [90] for the fuzzy controller and FOMCON Toolbox [91] for the design of the fractional order part of the FO-FPID controller. Especially to ensure for the software vs. hardware comparison accuracy, a 5th-order approximation for the fractional blocks is used for the software-based results too. Hardware implementation refers to the results from extracted/post-layout simulations of the FO-FPID controller circuit, conducted on the same plant (implemented with Verilog) within Cadence IC Virtuoso Suite.

The functional simulation of the proposed circuit topology has been performed through Cadence Virtuoso. All simulations are conducted on the implemented layout as shown in Figure 13. An analysis of the controller's time-domain performance was conducted by subjecting it to a step voltage with a magnitude of 150 mV. Then the extracted closed-loop system's response is scaled in order to compare it with the software-based equivalent. The resulting output waveform, juxtaposed with the corresponding theoretical response for the closed-loop controller-plant system, is depicted in Figure 14. The performance of both the software and hardware controllers are summarized in Table 4. Notably, the settling time of the controller was measured at 4.12 s, accompanied by an overshoot of 17.5%. The step response of the controller's output at unit-step reference is shown in Figure 15. It is imperative to acknowledge that the observed steady-state error in the comparison of the two responses in Figure 14 is attributable to imperfections in the OTAs and RC-network. These imperfections encompass non-linearities and finite output impedance, factors that contribute to the discernible disparities between the expected and actual outcomes. Regarding sensitivity analysis, a Monte-Carlo simulation was conducted comprising $N = 100$ runs and the results are displayed in Figure 16. We observe that the circuit exhibits a robust behavior with respect to process and mismatch random variations.

Table 4. Software-Hardware Fuzzy controller related metrics.

KPI	Software	Hardware
Rise time (10–90%)	0.54 s	0.67 s
Overshot	19.78%	17.45%
Settling time	3.97 s	4.12 s
Steady-state error	3.22%	3.74%

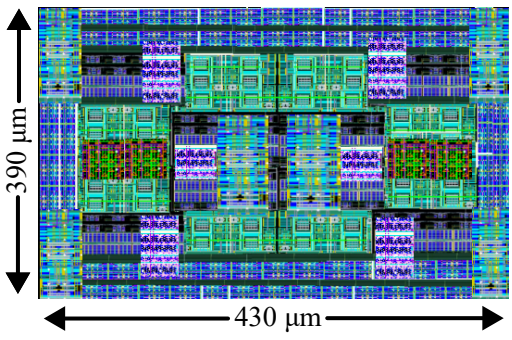

Figure 13. The layout implementation of the proposed analog FO-FPID controller on the TSMC 90 nm process node.

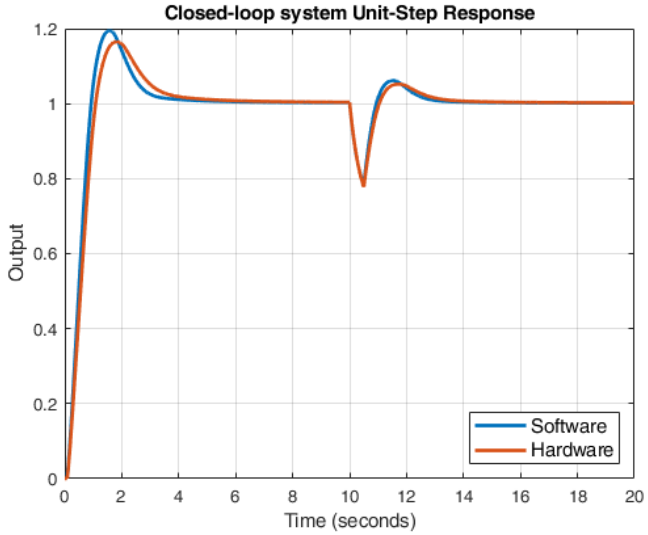

Figure 14. Step response of the closed-loop controller-plant system. It contains both software and hardware implementations.

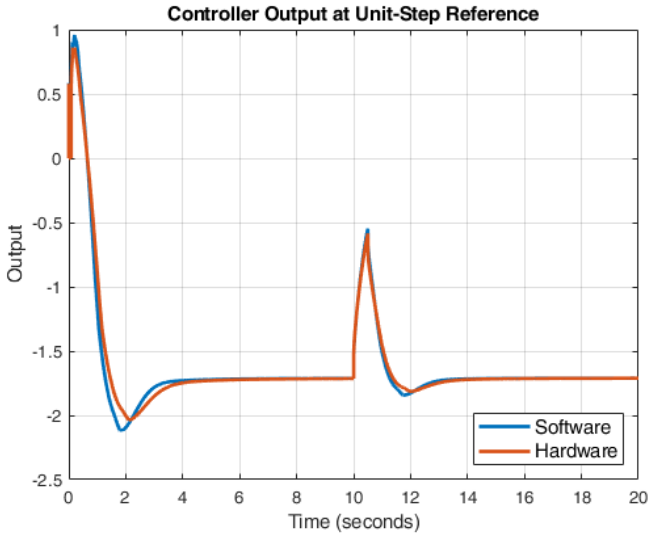

Figure 15. Step response of the controller's output at unit-step reference. It contains both software and hardware implementations.

As further proof of concept for the proper operation of the proposed analog implementation of the control system, the circuit is tested on a 2nd order non-linear plant, modelling the dynamics of the motion of a train on a track [92]. The differential equation representing the plant system is as follows

$$\ddot{y}(t) = -k\dot{y}(t) - r\dot{y}(t)|\dot{y}(t)| + u(t) \tag{12}$$

Likewise the 1st plant, in this case both a software (Matlab/Simulink) and the hardware-equivalent (post-layout simulation) controller have been tested to account for the analog implementation's efficiency and accuracy. The results for the closed-loop system's time step-response waveforms of the two implementations are illustrated in Figure 17 and the KPI values are summarized in Table 5. As in the 1st testcase small expected differences in the performance between software and hardware are explained within the contect of the intrinsic approximations and mismatches that the transistor-level implementation of mathematical models introduces.

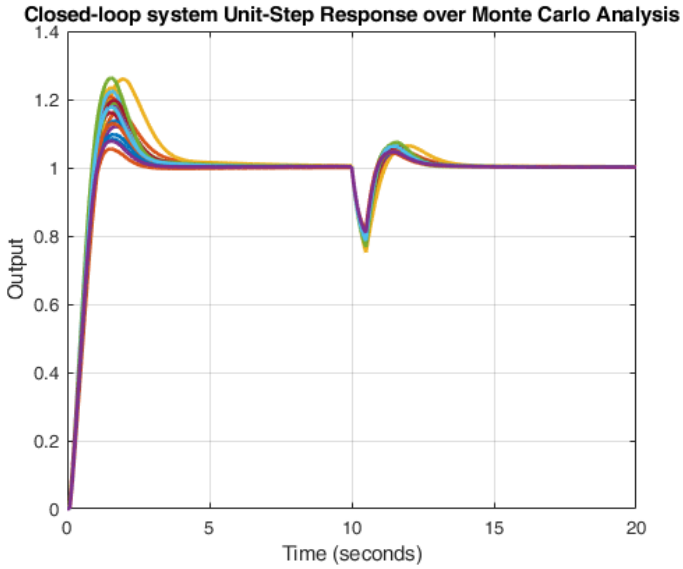

Figure 16. The hardware-implementation step response of the closed-loop system for a Monte Carlo Analysis with $N = 100$ points to test the robustness of the circuit.

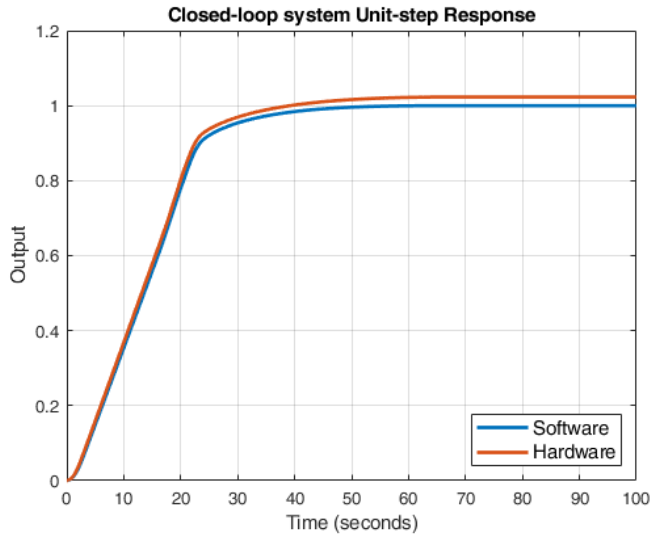

Figure 17. Step response of the closed-loop controller-plant system. It contains both software and hardware implementations.

Table 5. Software-Hardware Fuzzy controller related metrics.

KPI	Software	Hardware
Rise time (10–90%)	19.62 s	20.07 s
Overshot	0%	0%
Settling time	48.71 s	52.15 s
Steady-state error	0.11%	2.32%

6. Conclusions

This work introduces an integrated analog, low-power, tunable fuzzy PID controller with fractional-order design and explores its practical application. The suggested IC serves as a fundamental building block for developing advanced and intricate control systems. The design incorporates amplifiers/attenuators for the tunable control gains, CPEs for fractional operations, Bump circuits to generate Gaussian MFs, current-mode MIN/MAX circuits for fuzzy reasoning, and OTAs for defuzzification with COG approach. The proposed

controller's design was implemented with the Cadence IC Suite using a 90 nm TSMC process node and validated through post-layout simulations, showcasing a low power consumption of 861.8 nW. To ensure the correct performance of the system, a comparison with an equivalent software FO-FPID controller on the same plant was conducted.

Author Contributions: Investigation, V.A., N.P.E. and E.G.; writing—original draft, V.A., N.P.E., E.G. and C.D.; writing—review and editing, V.A., N.P.E., E.G., C.D., N.U. and P.P.S. All authors have read and agreed to the published version of the manuscript.

Funding: This research received no external funding.

Institutional Review Board Statement: Not applicable.

Informed Consent Statement: Not applicable.

Data Availability Statement: The raw data supporting the conclusions of this article will be made available by the authors on request.

Conflicts of Interest: The authors declare no conflict of interest.

References

1. Jang, H.; Topal, E. A review of soft computing technology applications in several mining problems. *Appl. Soft Comput.* **2014**, *22*, 638–651. [CrossRef]
2. Zadeh, L.A. Soft computing and fuzzy logic. *IEEE Softw.* **1994**, *11*, 48–56. [CrossRef]
3. Jang, J.; Sun, C.; Mizutani, E. *Neuro-Fuzzy and Soft Computing: A Computational Approach to Learning and Machine Intelligence*; MATLAB Curriculum Series; Prentice Hall: Upper Saddle River, NJ, USA, 1997.
4. Zadeh, L.A. Fuzzy sets. *Inf. Control* **1965**, *8*, 338–353. [CrossRef]
5. Seger, C.A.; Miller, E.K. Category learning in the brain. *Annu. Rev. Neurosci.* **2010**, *33*, 203–219. [CrossRef] [PubMed]
6. Smithson, M.; Verkuilen, J. *Fuzzy Set Theory: Applications in the Social Sciences*; Number 147; Sage: Newcastle upon Tyne, UK, 2006.
7. Pedrycz, W.; Gomide, F. *An Introduction to Fuzzy Sets: Analysis and Design*; MIT Press: Cambridge, MA, USA, 1998.
8. Klir, G.; Yuan, B. *Fuzzy Sets and Fuzzy Logic*; Prentice Hall: Upper Saddle River, NJ, USA, 1995; Volume 4.
9. Zadeh, L.A. A computational approach to fuzzy quantifiers in natural languages. In *Computational Linguistics*; Elsevier: Amsterdam, The Netherlands, 1983; pp. 149–184.
10. Shihabudheen, K.; Pillai, G.N. Recent advances in neuro-fuzzy system: A survey. *Knowl.-Based Syst.* **2018**, *152*, 136–162.
11. Carvajal, J.; Chen, G.; Ogmen, H. Fuzzy PID controller: Design, performance evaluation, and stability analysis. *Inf. Sci.* **2000**, *123*, 249–270. [CrossRef]
12. Nguyen, H.T.; Prasad, N.R.; Walker, C.L.; Walker, E.A. *A First Course in Fuzzy and Neural Control*; CRC Press: Boca Raton, FL, USA, 2002.
13. Jerry, M.M. *Uncertain Rule-Based Fuzzy Systems: Introduction and New Directions*; Springer: Berlin, Germany, 2019.
14. Jantzen, J. *Foundations of Fuzzy Control: A Practical Approach*; John Wiley & Sons: Hoboken, NJ, USA, 2013.
15. Al-Odienat, A.I.; Al-Lawama, A.A. The advantages of PID fuzzy controllers over the conventional types. *Am. J. Appl. Sci.* **2008**, *5*, 653–658. [CrossRef]
16. Haensch, W.; Gokmen, T.; Puri, R. The next generation of deep learning hardware: Analog computing. *Proc. IEEE* **2018**, *107*, 108–122. [CrossRef]
17. Bonissone, P.P.; Badami, V.; Chiang, K.H.; Khedkar, P.S.; Marcelle, K.W.; Schutten, M.J. Industrial applications of fuzzy logic at General Electric. *Proc. IEEE* **1995**, *83*, 450–465. [CrossRef]
18. Sun, H.; Zhao, H.; Huang, K.; Qiu, M.; Zhen, S.; Chen, Y.H. A fuzzy approach for optimal robust control design of an automotive electronic throttle system. *IEEE Trans. Fuzzy Syst.* **2017**, *26*, 694–704. [CrossRef]
19. Li, C.; Hu, R. Fuzzy-PID control for the regulation of blood glucose in diabetes. In Proceedings of the 2009 WRI Global Congress on Intelligent Systems, Xiamen, China, 19–21 May 2009; Volume 2, pp. 170–174.
20. Kapoulea, S.; Yesil, A.; Psychalinos, C.; Minaei, S.; Elwakil, A.S.; Bertsias, P. Fractional-order and power-law shelving filters: Analysis and design examples. *IEEE Access* **2021**, *9*, 145977–145987. [CrossRef]
21. Sacu, I.E.; Alci, M. Low-power OTA-C based tuneable fractional order filters. *Electron. Components Mater.* **2018**, *48*, 135–144.
22. Valencia-Ponce, M.A.; González-Zapata, A.M.; de la Fraga, L.G.; Sanchez-Lopez, C.; Tlelo-Cuautle, E. Integrated Circuit Design of Fractional-Order Chaotic Systems Optimized by Metaheuristics. *Electronics* **2023**, *12*, 413. [CrossRef]
23. Bertsias, P.; Safari, L.; Minaei, S.; Elwakil, A.; Psychalinos, C. Fractional-order differentiators and integrators with reduced circuit complexity. In Proceedings of the 2018 IEEE International Symposium on Circuits and Systems (ISCAS), Florence, Italy, 27–30 May 2018; pp. 1–4.
24. Tsirimokou, G.; Psychalinos, C.; Elwakil, A.S.; Salama, K.N. Electronically tunable fully integrated fractional-order resonator. *IEEE Trans. Circuits Syst. II Express Briefs* **2017**, *65*, 166–170. [CrossRef]

25. Sharma, R.; Rana, K.; Kumar, V. Performance analysis of fractional order fuzzy PID controllers applied to a robotic manipulator. *Expert Syst. Appl.* **2014**, *41*, 4274–4289. [CrossRef]
26. Mohan, V.; Panjwani, B.; Chhabra, H.; Rani, A.; Singh, V. Self-regulatory fractional fuzzy control for dynamic systems: An analytical approach. *Int. J. Fuzzy Syst.* **2023**, *25*, 794–815. [CrossRef]
27. Matusu, R. Application of fractional order calculus to control theory. *Int. J. Math. Model. Methods Appl. Sci.* **2011**, *5*, 1162–1169.
28. Delavari, H.; Ghaderi, R.; Ranjbar, A.; Momani, S. Fuzzy fractional order sliding mode controller for nonlinear systems. *Commun. Nonlinear Sci. Numer. Simul.* **2010**, *15*, 963–978. [CrossRef]
29. Yen, J. *Fuzzy Logic: Intelligence, Control, and Information*; Pearson Education: Noida, India, 1999.
30. Yang, Q.; Yao, D.; Garnett, J.; Muller, K. Using a trust inference model for flexible and controlled information sharing during crises. *J. Contingencies Crisis Manag.* **2010**, *18*, 231–241. [CrossRef]
31. Al-Turki, Y.A.; Attia, A.F.; Soliman, H.F. Optimization of fuzzy logic controller for supervisory power system stabilizers. *Acta Polytech.* **2012**, *52*, 7–16. [CrossRef]
32. Arya, Y. A new optimized fuzzy FOPI-FOPD controller for automatic generation control of electric power systems. *J. Frankl. Inst.* **2019**, *356*, 5611–5629. [CrossRef]
33. Arya, Y. Automatic generation control of two-area electrical power systems via optimal fuzzy classical controller. *J. Frankl. Inst.* **2018**, *355*, 2662–2688. [CrossRef]
34. Liu, J.; Yang, O.W. Using fuzzy logic control to provide intelligent traffic management service for high-speed networks. *IEEE Trans. Netw. Serv. Manag.* **2013**, *10*, 148–161.
35. Islam, M.S.; Bhuyan, M.; Azim, M.A.; Teng, L.; Othman, M. Hardware implementation of traffic controller using fuzzy expert system. In Proceedings of the 2006 International Symposium on Evolving Fuzzy Systems, Ambelside, UK, 7–9 September 2006; pp. 325–330.
36. Madrigal Arteaga, V.M.; Pérez Cruz, J.R.; Hurtado-Beltrán, A.; Trumpold, J. Efficient Intersection Management Based on an Adaptive Fuzzy-Logic Traffic Signal. *Appl. Sci.* **2022**, *12*, 6024. [CrossRef]
37. Sánchez-Solano, S.; Cabrera, A.J.; Baturone, I.; Moreno-Velo, F.J.; Brox, M. FPGA implementation of embedded fuzzy controllers for robotic applications. *IEEE Trans. Ind. Electron.* **2007**, *54*, 1937–1945. [CrossRef]
38. Silva, S.N.; Lopes, F.F.; Valderrama, C.; Fernandes, M.A. Proposal of Takagi–Sugeno fuzzy-PI controller hardware. *Sensors* **2020**, *20*, 1996. [CrossRef]
39. Varshavsky, V.; Marakhovsky, V.; Levin, I.; Saito, H. Hardware Implementation of Fuzzy Controllers. In *Fuzzy Controller, Theory and Applications*; In-Tech: Rijeka, Croatia, 2011; pp. 34–44.
40. Uzunsoy, E. A brief review on fuzzy logic used in vehicle dynamics control. *J. Innov. Sci. Eng. (JISE)* **2018**, *2*, 1–7.
41. Wang, Z.; Choi, S.B. A fuzzy sliding mode control of anti-lock system featured by magnetorheological brakes: Performance evaluation via the hardware-in-the-loop simulation. *J. Intell. Mater. Syst. Struct.* **2021**, *32*, 1580–1590. [CrossRef]
42. Rubaai, A.; Ofoli, A.R.; Burge, L.; Garuba, M. Hardware implementation of an adaptive network-based fuzzy controller for DC-DC converters. *IEEE Trans. Ind. Appl.* **2005**, *41*, 1557–1565. [CrossRef]
43. Bosque, G.; del Campo, I.; Echanobe, J. Fuzzy systems, neural networks and neuro-fuzzy systems: A vision on their hardware implementation and platforms over two decades. *Eng. Appl. Artif. Intell.* **2014**, *32*, 283–331. [CrossRef]
44. Kuo, Y.H.; Kao, C.I.; Chen, J.J. A fuzzy neural network model and its hardware implementation. *IEEE Trans. Fuzzy Syst.* **1993**, *1*, 171–183. [CrossRef]
45. Lotfy, A.; Kaveh, M.; Mosavi, M.; Rahmati, A. An enhanced fuzzy controller based on improved genetic algorithm for speed control of DC motors. *Analog. Integr. Circuits Signal Process.* **2020**, *105*, 141–155. [CrossRef]
46. Herrera, F.; Lozano, M.; Verdegay, J.L. Tuning fuzzy logic controllers by genetic algorithms. *Int. J. Approx. Reason.* **1995**, *12*, 299–315. [CrossRef]
47. Khan, S.; Abdulazeez, S.F.; Adetunji, L.W.; Alam, A.Z.; Salami, M.J.E.; Hameed, S.A.; Abdalla, A.H.; Islam, M.R. Design and implementation of an optimal fuzzy logic controller using genetic algorithm. *J. Comput. Sci.* **2008**, *4*, 799. [CrossRef]
48. Caponetto, R.; Dongola, G.; Maione, G.; Pisano, A. Integrated technology fractional order proportional-integral-derivative design. *J. Vib. Control.* **2014**, *20*, 1066–1075. [CrossRef]
49. Tepljakov, A.; Petlenkov, E.; Belikov, J. Efficient analog implementations of fractional-order controllers. In Proceedings of the 14th International Carpathian Control Conference (ICCC), Rytro, Poland, 26–29 May 2013; pp. 377–382.
50. Psychalinos, C. Development of fractional-order analog integrated controllers—Application examples. *Appl. Control* **2019**, *6*, 357.
51. Muñiz-Montero, C.; García-Jiménez, L.V.; Sánchez-Gaspariano, L.A.; Sánchez-López, C.; González-Díaz, V.R.; Tlelo-Cuautle, E. New alternatives for analog implementation of fractional-order integrators, differentiators and PID controllers based on integer-order integrators. *Nonlinear Dyn.* **2017**, *90*, 241–256. [CrossRef]
52. Podlubny, I.; Petráš, I.; Vinagre, B.M.; O'Leary, P.; Dorčák, L. Analogue realizations of fractional-order controllers. *Nonlinear Dyn.* **2002**, *29*, 281–296. [CrossRef]
53. Bohannan, G.W. Analog fractional order controller in temperature and motor control applications. *J. Vib. Control.* **2008**, *14*, 1487–1498. [CrossRef]
54. Petráš, I. Fractional-order feedback control of a DC motor. *J. Electr. Eng.* **2009**, *60*, 117–128.
55. Mokarram, M.; Khoei, A.; Hadidi, K. CMOS fuzzy logic controller supporting fractional polynomial membership functions. *Fuzzy Sets Syst.* **2015**, *263*, 112–126. [CrossRef]

56. Johnson, M.A.; Moradi, M.H. *PID Control*; Springer: Berlin, Germany, 2005.
57. Mousa, M.; Ebrahim, M.A.; Moustafa Hassan, M. Optimal fractional order proportional—integral—differential controller for inverted pendulum with reduced order linear quadratic regulator. In *Fractional Order Control and Synchronization of Chaotic Systems*; Springer: Berlin, Germany, 2017; pp. 225–252.
58. Jamil, A.A.; Tu, W.F.; Ali, S.W.; Terriche, Y.; Guerrero, J.M. Fractional-order PID controllers for temperature control: A review. *Energies* **2022**, *15*, 3800. [CrossRef]
59. Shah, P.; Agashe, S. Review of fractional PID controller. *Mechatronics* **2016**, *38*, 29–41. [CrossRef]
60. Bingi, K.; Ibrahim, R.; Karsiti, M.N.; Hassan, S.M.; Harindran, V.R. *Fractional-Order Systems and PID Controllers*; Springer: Berlin, Germany, 2020; Volume 264.
61. Sivanandam, S.; Sumathi, S.; Deepa, S. *Introduction to Fuzzy Logic Using MATLAB*; Springer: Berlin, Germany, 2007.
62. Mamdani, E.H.; Assilian, S. An experiment in linguistic synthesis with a fuzzy logic controller. *Int. J.-Man-Mach. Stud.* **1975**, *7*, 1–13. [CrossRef]
63. Pan, I.; Das, S.; Gupta, A. Tuning of an optimal fuzzy PID controller with stochastic algorithms for networked control systems with random time delay. *ISA Trans.* **2011**, *50*, 28–36. [CrossRef]
64. Barakat, M. Optimal design of fuzzy-PID controller for automatic generation control of multi-source interconnected power system. *Neural Comput. Appl.* **2022**, *34*, 18859–18880. [CrossRef]
65. Das, S.; Pan, I.; Das, S.; Gupta, A. A novel fractional order fuzzy PID controller and its optimal time domain tuning based on integral performance indices. *Eng. Appl. Artif. Intell.* **2012**, *25*, 430–442. [CrossRef]
66. Buscarino, A.; Caponetto, R.; Graziani, S.; Murgano, E. Realization of fractional order circuits by a Constant Phase Element. *Eur. J. Control* **2020**, *54*, 64–72. [CrossRef]
67. Abdelliche, F.; Charef, A.; Talbi, M.; Benmalek, M. A fractional wavelet for QRS detection. In Proceedings of the 2006 2nd International Conference on Information & Communication Technologies, Damascus, Syria, 24–28 April 2006; Volume 1, pp. 1186–1189.
68. Benmalek, M.; Charef, A. Digital fractional order operators for R-wave detection in electrocardiogram signal. *IET Signal Process.* **2009**, *3*, 381–391. [CrossRef]
69. Li, B.; Wu, J. Beta-expansion and continued fraction expansion. *J. Math. Anal. Appl.* **2008**, *339*, 1322–1331. [CrossRef]
70. Chen, Y.; Vinagre, B.M.; Podlubny, I. Continued fraction expansion approaches to discretizing fractional order derivatives—An expository review. *Nonlinear Dyn.* **2004**, *38*, 155–170. [CrossRef]
71. Colín-Cervantes, J.D.; Sánchez-López, C.; Ochoa-Montiel, R.; Torres-Muñoz, D.; Hernández-Mejía, C.M.; Sánchez-Gaspariano, L.A.; González-Hernández, H.G. Rational approximations of arbitrary order: A survey. *Fractal Fract.* **2021**, *5*, 267. [CrossRef]
72. Tavazoei, M.S.; Haeri, M. Rational approximations in the simulation and implementation of fractional-order dynamics: A descriptor system approach. *Automatica* **2010**, *46*, 94–100. [CrossRef]
73. Tsirimokou, G. A systematic procedure for deriving RC networks of fractional-order elements emulators using MATLAB. *AEU Int. J. Electron. Commun.* **2017**, *78*, 7–14. [CrossRef]
74. Acay, B.; Inc, M. Electrical circuits RC, LC, and RLC under generalized type non-local singular fractional operator. *Fractal Fract.* **2021**, *5*, 9. [CrossRef]
75. Lin, D.; Liao, X.; Dong, L.; Yang, R.; Samson, S.Y.; Iu, H.H.C.; Fernando, T.; Li, Z. Experimental study of fractional-order RC circuit model using the Caputo and Caputo-Fabrizio derivatives. *IEEE Trans. Circuits Syst. I Regul. Pap.* **2021**, *68*, 1034–1044. [CrossRef]
76. Sen, F.; Kircay, A.; Cobb, B.S.; Karci, H. Current-mode fractional-order shelving filters using MCFOA for acoustic applications. *AEU Int. J. Electron. Commun.* **2023**, *163*, 154608. [CrossRef]
77. Kartci, A.; Herencsar, N.; Machado, J.T.; Brancik, L. History and progress of fractional-order element passive emulators: A review. *Radioengineering* **2020**, *29*, 296–304. [CrossRef]
78. Alimisis, V.; Dimas, C.; Pappas, G.; Sotiriadis, P.P. Analog realization of fractional-order skin-electrode model for tetrapolar bio-impedance measurements. *Technologies* **2020**, *8*, 61. [CrossRef]
79. Alimisis, V.; Mouzakis, V.; Gennis, G.; Tsouvalas, E.; Sotiriadis, P.P. An Analog Nearest Class with Multiple Centroids Classifier Implementation, for Depth of Anesthesia Monitoring. In Proceedings of the 2022 International Conference on Smart Systems and Power Management (IC2SPM), Beirut, Lebanon, 10–12 November 2022; pp. 176–181.
80. Alimisis, V.; Eleftheriou, N.P.; Kamperi, A.; Gennis, G.; Dimas, C.; Sotiriadis, P.P. General Methodology for the Design of Bell-Shaped Analog-Hardware Classifiers. *Electronics* **2023**, *12*, 4211. [CrossRef]
81. Dualibe, C.; Verleysen, M.; Jespers, P. *Design of Analog Fuzzy Logic Controllers in CMOS Technologies: Implementation, Test and Application*; Springer Science & Business Media: Berlin, Germany, 2007.
82. Sánchez-Gaspariano, L.A.; Díaz-Sánchez, A. CMOS Analog MAX/MIN operators: A qualitative comparsion. In Proceedings of the XV Congreso Interuniversitario de Electrónica, Computación y Eléctrica, Puebla, Mexico, 7–9 March 2005; pp. 7–9.
83. Georgakilas, E.; Alimisis, V.; Gennis, G.; Aletraris, C.; Dimas, C.; Sotiriadis, P.P. An ultra-low power fully-programmable analog general purpose type-2 fuzzy inference system. *AEU Int. J. Electron. Commun.* **2023**, *170*, 154824. [CrossRef]
84. Alikhani, A.; Ahmadi, A. A novel current-mode min–max circuit. *Analog. Integr. Circuits Signal Process.* **2012**, *72*, 343–350. [CrossRef]
85. Baturone, I.; Sánchez-Solano, S.; Barriga, A.; Huertas, J. Implementation of inference/defuzzification methods via continuous-time analog circuits. In Proceedings of the IFSA World Congress, Sao Paulo, Brasil, 22–28 July 1995; pp. 623–626.

86. Daneshvar, M.; Aminifar, S.; Yosefi, G. Design and Analysis of Current-Mode CMOS Analog Defuzzification Circuits for Fuzzy Controllers. *J. Basic. Appl. Sci. Res.* **2011**, *1*, 2488–2494.
87. Mead, C.; Ismail, M. *Analog VLSI Implementation of Neural Systems*; Springer Science & Business Media: Berlin, Germany, 1989; Volume 80.
88. Columbu, A.; Frassu, S.; Viglialoro, G. Properties of given and detected unbounded solutions to a class of chemotaxis models. *arXiv* **2023**, arXiv:2303.15039.
89. Kumar, A.; Kumar, V. A novel interval type-2 fractional order fuzzy PID controller: Design, performance evaluation, and its optimal time domain tuning. *ISA Trans.* **2017**, *68*, 251–275. [CrossRef]
90. Fuzzy Logic Toolbox. Available online: https://www.mathworks.com/products/fuzzy-logic.html (accessed on 10 December 2023).
91. FOMCON Toolbox. Available online: https://www.mathworks.com/matlabcentral/fileexchange/66323-fomcon-toolbox-for-matlab (accessed on 10 December 2023).
92. Cunillera, A.; Bešinović, N.; Lentink, R.M.; van Oort, N.; Goverde, R.M. A Literature Review on Train Motion Model Calibration. *IEEE Trans. Intell. Transp. Syst.* **2023**, *24*, 3660–3677. [CrossRef]